

AD-A195 061

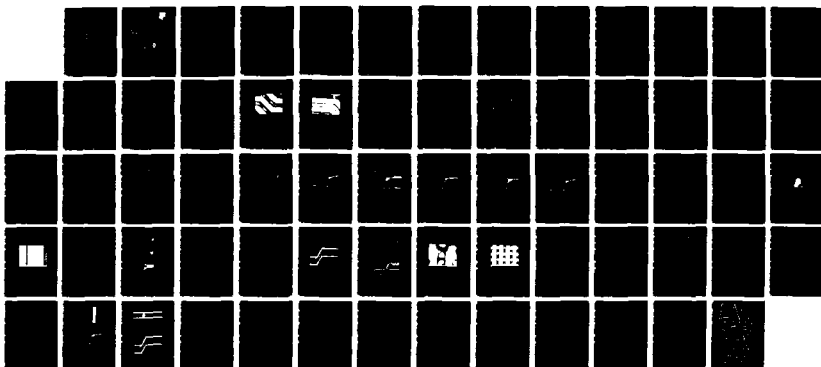
STRESS RELATED FAILURES CAUSING OPEN METALLIZATION(U)
TEXAS INSTRUMENTS INC DALLAS SEMICONDUCTOR GROUP
S K GROOTHUIS JAN 88 RADC-RR-88-8 F30602-85-C-0093

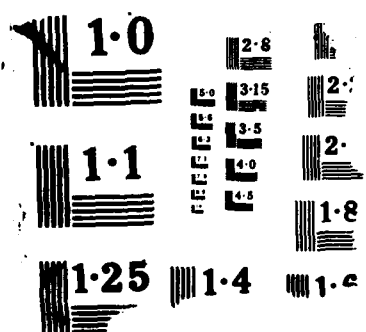
1/1

UNCLASSIFIED

F/G 11/3

NL





DTIC FILE COPY

4

AD-A195 061

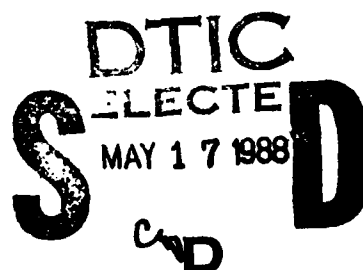
RADC-TR-88-8
Final Technical Report
January 1988



STRESS RELATED FAILURES CAUSING OPEN METALLIZATION

Texas Instruments Incorporated

Steven K. Groothuis



APPROVED FOR PUBLIC RELEASE; DISTRIBUTION UNLIMITED

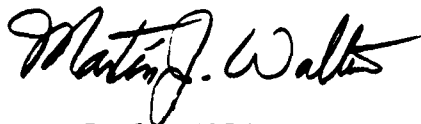
ROME AIR DEVELOPMENT CENTER
Air Force Systems Command
Griffiss Air Force Base, NY 13441-5700

88 5 16 06 9

This report has been reviewed by the RADC Public Affairs Office (PA) and is releasable to the National Technical Information Service (NTIS). At NTIS it will be releasable to the general public, including foreign nations.

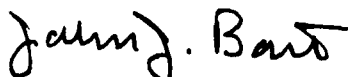
RADC-TR-88-8 has been reviewed and is approved for publication.

APPROVED:



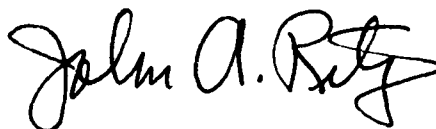
MARTIN J. WALTER
Project Engineer

APPROVED:



JOHN J. BART
Technical Director
Directorate of Reliability & Compatibility

FOR THE COMMANDER:



JOHN A. RITZ
Directorate of Plans & Programs

If your address has changed or if you wish to be removed from the RADC mailing list, or if the addressee is no longer employed by your organization, please notify RADC (RBRP) Griffiss AFB NY 13441-5700. This will assist us in maintaining a current mailing list.

Do not return copies of this report unless contractual obligations or notice on a specific document requires that it be returned.

REPORT DOCUMENTATION PAGE				Form Approved OMB No. 0704-0188	
1a. REPORT SECURITY CLASSIFICATION UNCLASSIFIED			1b. RESTRICTIVE MARKINGS N/A		
2a. SECURITY CLASSIFICATION AUTHORITY N/A			3. DISTRIBUTION / AVAILABILITY OF REPORT Approved for public release; distribution unlimited.		
2b. DECLASSIFICATION / DOWNGRADING SCHEDULE N/A					
4. PERFORMING ORGANIZATION REPORT NUMBER(S) N/A			5. MONITORING ORGANIZATION REPORT NUMBER(S) RADC-TR-88-8		
6a. NAME OF PERFORMING ORGANIZATION Texas Instruments Incorporated		6b. OFFICE SYMBOL (if applicable)	7a. NAME OF MONITORING ORGANIZATION Rome Air Development Center (RBRP)		
6c. ADDRESS (City, State, and ZIP Code) Semiconductor Group P.O. Box 655012, M/S477 Dallas TX 75265			7b. ADDRESS (City, State, and ZIP Code) Griffiss AFB NY 13441-5700		
8a. NAME OF FUNDING / SPONSORING ORGANIZATION Rome Air Development Center		8b. OFFICE SYMBOL (if applicable) RBRP	9. PROCUREMENT INSTRUMENT IDENTIFICATION NUMBER F30602-85-C-0093		
8c. ADDRESS (City, State, and ZIP Code) Griffiss AFB NY 13441-5700			10. SOURCE OF FUNDING NUMBERS		
			PROGRAM ELEMENT NO. 62702F	PROJECT NO. 2338	TASK NO. 01
11. TITLE (Include Security Classification) STRESS RELATED FAILURES CAUSING OPEN METALLIZATION					
12. PERSONAL AUTHOR(S) Steven K. Groothuis					
13a. TYPE OF REPORT Final		13b. TIME COVERED FROM Jun 85 TO Jul 87		14. DATE OF REPORT (Year, Month, Day) January 1988	
15. PAGE COUNT 80					
16. SUPPLEMENTARY NOTATION N/A					
17. COSATI CODES			18. SUBJECT TERMS (Continue on reverse if necessary and identify by block number)		
FIELD	GROUP	SUB-GROUP	Modeling ,		
20	12		Stress		
			Finite Element Analysis ,		
			Thin Films ,		
			Voids ,		
			Conductors		
19. ABSTRACT (Continue on reverse if necessary and identify by block number)					
<p>Non-linear Finite Element Analysis has been used to model stresses and infer stress induced void formation in narrow Al-S; metal lines. Observed failures correlate well with calculated stresses determined by varying intrinsic stress of the passivation, topography, line width and silicon nodule size.</p> <p><i>Responsible: Aluminum, Silicon</i></p>					
20. DISTRIBUTION / AVAILABILITY OF ABSTRACT <input checked="" type="checkbox"/> UNCLASSIFIED/UNLIMITED <input type="checkbox"/> SAME AS RPT <input type="checkbox"/> DTIC USERS			21. ABSTRACT SECURITY CLASSIFICATION UNCLASSIFIED		
22a. NAME OF RESPONSIBLE INDIVIDUAL Martin J. Walter			22b. TELEPHONE (Include Area Code) (315) 330-4995		22c. OFFICE SYMBOL RADC (RBRP)

UNCLASSIFIED

UNCLASSIFIED

EVALUATION

This contract resulted from a Program Research and Development Announcement on Failure Mechanisms in VLSI. Texas Instruments investigated the role of stresses in thin metal conductors by use of finite element analysis. The programs used for this analysis were already in existence at TI and similar programs are available commercially. This work has been pioneering in the area of thin film conductor reliability, and has been published in the Proceedings of the 1987 International Reliability Physics Symposium. Similar work was being conducted at INMOS, and was also reported in the same Proceedings.

The report addresses the effects of topography and material properties on stresses within an Al-Si conductor film. There is a good correlation between the calculated maximum stress as a function of linewidth and the density of voids as a function of linewidth reported in the 1985 IRPS. These calculations do not address the evolution of void growth, or silicon precipitate growth. They are a method of evaluating the initial driving forces present, and how those forces are modified by topology and macroscopic material properties. Areas which remain to be investigated include the metal spacing, the height of a step, corners, and interactions between combinations of these effects.

Martin J. Walter
MARTIN J. WALTER
Project Engineer



Accession For	
NTIS CRA&I	<input checked="" type="checkbox"/>
DTIC TAB	<input type="checkbox"/>
Unannounced	<input type="checkbox"/>
Justification	
By	
Date	
Availability Codes	
1	
A-1	

TABLE OF CONTENTS

<u>Section</u>	<u>Title</u>	<u>Page</u>
1.0	BACKGROUND	1
2.0	INTRODUCTION	3
3.0	THERMOMECHANICAL STRESS THEORY	7
3.1	Stress and vacancy concentration	10
3.2	Stress enhanced vacancy diffusion	11
4.0	MODELING RESULTS	15
4.1	Finite element modeling fundamentals	15
4.2	Application of finite element modeling	16
4.3	Effects of underlying oxide layer	19
4.4	Linewidth dependence of stress	19
4.5	Compressive stress passivation layer	27
4.6	Silicon nodules	28
4.7	Metallization parameters	34
4.7.1	Metal line topography	34
4.7.2	Variations in metal thickness	34
4.7.3	Metallization yield strength variations	40

TABLE OF CONTENTS
(Continued)

<u>Section</u>	<u>Title</u>	<u>Page</u>
	4.7.4 Metal line slant angle . . .	40
4.8	Aluminum-copper metal systems . . .	40
4.9	Three dimensional effects	40
5.0	SUMMARY AND CONCLUSIONS	49
6.0	RECOMMENDATIONS	53
	REFERENCES	55
	APPENDIX -- STRESS CALCULATIONS	59

APPENDIX

STRESS CALCULATIONS

1.0 GENERAL ASSUMPTIONS

The physical stress model of a passivated Al-Si metal line is representative of single level interconnect systems in current integrated circuits. Line widths from 1 to 10 microns were investigated for a typical system of a 1 micron Al-Si line on a 0.5 micron thick layer of silicon dioxide over a silicon wafer with 1 micron of compressive silicon nitride passivation.

1.1 Temperature boundary conditions

The temperature at which every material was at zero stress was assumed to be 400 degrees C. To a first order approximation, this assumption is believed to be valid. Additional features which can lead to a more accurate model would be thermal stress history of the metallization (i.e., annealing, any high temperature excursion, gold eutectic die attach, etc.). The stresses were then investigated as a function of cooling down to 25 degrees C.

1.2 Material properties

The material properties used for the analysis are listed in Table A-1 and are fairly representative of literature values. This table has evolved from several sources and a similar finite element stress modeling study performed by Jones [10]. The room temperature yield strength of the Al-Si metallization was modeled to be approximately 100 MPascals. The characteristic stress distribution calculated during this project is expected not to vary significantly with material variations.

1.3 Analysis tools

The nonlinear finite element software (ADINA) used for this analysis was selected for its general purpose elastic-plastic features of material properties as a function of thermal loads. Several other finite element modeling codes do exist which perform in the same manner.

TABLE A-1. TEMPERATURE-DEPENDENT MATERIAL PROPERTIES

MATERIAL	TEMPERATURE (DEGREE C)				
	25	100	200	300	400
PROPERTY : MODULUS OF ELASTICITY (GPascals)					
Al-Si	69	68	62	49	40
Silicon	130	130	130	130	130
Si3N4	90	90	90	90	90
SiO2	80	80	80	80	80
PROPERTY : THERMAL COEF. OF EXPANSION (ppm/deg C)					
Al-Si	24.0	24.0	26.0	29.0	30.0
Silicon	2.3	2.9	3.4	3.8	4.0
Si3N4	2.2	2.8	3.5	4.1	4.3
SiO2	0.5	0.7	1.1	1.5	1.7
PROPERTY : YIELD STRENGTH (MPascals)					
Al-Si	100	100	70	30	15

LIST OF FIGURES

<u>Figure No.</u>	<u>Title</u>	<u>Page</u>
1.	Metal voids observed in narrow Al-Si interconnects (SEM, after passivation removal).	4
2.	Half of cross sectional area restricted by metal void (SEM, after passivation removal).	5
3.	Schematic of vacancy flow within a grain experiencing tensile stress.	9
4.	Finite element mesh describing stress model geometry.	18
5.	Von Mises stress contour plot for 1 micron wide Al-Si metal (contours at every 50 MPa).	20
6.	Von Mises stress contour plot for 2 micron wide Al-Si metal (contours at every 50 MPa).	21
7.	Von Mises stress contour plot for 3 micron wide Al-Si metal (contours at every 50 MPa).	22
8.	Von Mises stress contour plot for 5 micron wide Al-Si metal (contours at every 50 MPa).	23
9.	Von Mises stress contour plot for 10 micron wide Al-Si metal (contours at every 50 MPa).	24
10.	Typical location for maximum von Mises stress in Al-Si metallization (contours at every 50 MPa).	25
11.	Comparison of theoretical stress modeling values to experimental observations ²	26

LIST OF FIGURES
(Continued)

<u>Figure No.</u>	<u>Title</u>	<u>Page</u>
12.	Maximum tensile stress contour plot for 5 micron wide Al-Si metal with presence of a silicon nodule (contours at every 50 MPa).	29
13.	Proximity effect of silicon nodule and metal void formation (SEM, partially etched metallization).	30
14.	Induced Stress for Several Silicon Nodule Sizes (contours at every 50 MPa) . .	32
15.	Maximum Tensile and Von Mises Stress as a Function of Silicon Nodule Size-to-Linewidth Ratio.	33
16.	Maximum principal stress contour plot for Al-Si metal traversing over 1 micron oxide step (contours at every 50 MPa). . .	35
17a.	Von Mises stress contour plot for 3 micron wide Al-Si metal on flat surface (contours at every 50 MPa).	36
17b.	Von Mises stress contour plot for Al-Si metal traversing over 1 micron oxide step (contours at every 50 MPa).	36
18.	Metal voids observed in narrow Al-Si interconnects at oxide step (SEM, after passivation removal).	37
19.	Metal void formation adjacent to oxide step (SEM, after passivation removal). . .	38
20.	Maximum Von Mises Stress as a Function of Several Linewidths and Thicknesses. . .	39
21.	Induced Stress for Several Yield Strengths of Al-Si Metallization (von Mises Stress) (contours at every 50 MPa).	41

LIST OF FIGURES
(Continued)

<u>Figure No.</u>	<u>Title</u>	<u>Page</u>
22.	Maximum Von Mises Stress as a Function of Metal Yield Strength (for a 3 micron wide metal line).	42
23.	Induced Stress for Several Slant Angles of Al-Si Metallization Edge (contours at every 50 MPa).	43
24.	Three Dimensional View of Metallization Stress.	45
25.	Three Dimensional View of Metallization Stress Over an Oxide Step.	46

LIST OF TABLES

<u>Table No.</u>	<u>Title</u>	<u>Page</u>
1.	Typical Material Properties	7
A-1.	Temperature-dependent Material Properties.	60

ACKNOWLEDGEMENTS

This work was supported by Air Force Systems Command, Rome Air Development Center, Griffiss Air Force Base, New York under Contract No. F30602-85-C-0093. The authors gratefully acknowledge Joe McPherson, Clyde Dunn, and P.B. Ghate of Texas Instruments for their experimental data and discussions.

We also acknowledge Martin Walter of RADC for his technical support throughout the program.

1.0 BACKGROUND

With the ever increasing number of metallization failures caused by voids and subsequent opens, the reliability of narrow Al-Si metal lines has become a crucial factor in very large scale integration (VLSI) device fabrication and assembly. The only supporting evidence for void formation in the recent past has been visual inspection of failed open metallization. The open metallization failure rate increases as the passivation thickness increases, the metal line becomes narrower and thinner, and as the mean grain size of the metallization increases.

When thin film metallizations are stressed by an amount smaller than the elastic limit, they deform elastically and return to their original shape after the stress is relieved. However, when the stress is beyond the elastic limit, the films deform plastically and do not return to the original shape after the stress is relieved. The plastic deformation usually deteriorates the mechanical properties of the thin films. It is that plastic deformation that is the primary cause of void formation in compressively passivated Al-Si metallization.

Stress-induced void formation can be modeled using nonlinear finite element analysis. Theoretically calculated stresses have correlated well with observed failures. The stresses modeled during this contract were a function of varying intrinsic stress of passivation layers, metallization topography, line width, and silicon nodule size.

2.0 INTRODUCTION

The purpose of this work is to determine the stress distribution and the probability of void formation in Al-Si metallization through the use of finite element modeling (FEM). Although all parameters which constitute the actual stress in the metallization have not been used, the characteristics of the stress distribution in the metallization lend a simple physical interpretation of the void formation mechanism. The variables used are as follows :

- (1) Al-Si line widths
- (2) Magnitude of compressive stress
in passivation layer
- (3) Presence of silicon nodules
- (4) Metal line topography

Formation of voids within Al-Si metallization has been reported after passivation deposition [1,2], high temperature IC fabrication processes [3], and aging tests [4,5]. The associated reliability implications of metal void and silicon nodule formation are as follows : significant reduction in net metal line cross-sectional area, rise in local current density, and thereby increased probability of failure due to electromigration or localized heating, and loss of continuity due to subsequent microscopic cracks in the metal line. Two typical types of voids can be seen in Figures 1 and 2.

Several factors which influence the void formation and are relatively difficult to model will not be reported in this paper. These factors include the addition of small percentage of copper to the Al-Si alloy [1], infrared radiation of passivation [6], nitrogen content [7], and grain size / orientation [8,9].



Figure 1. Metal voids observed in narrow Al-Si interconnects (SEM, after passivation removal).

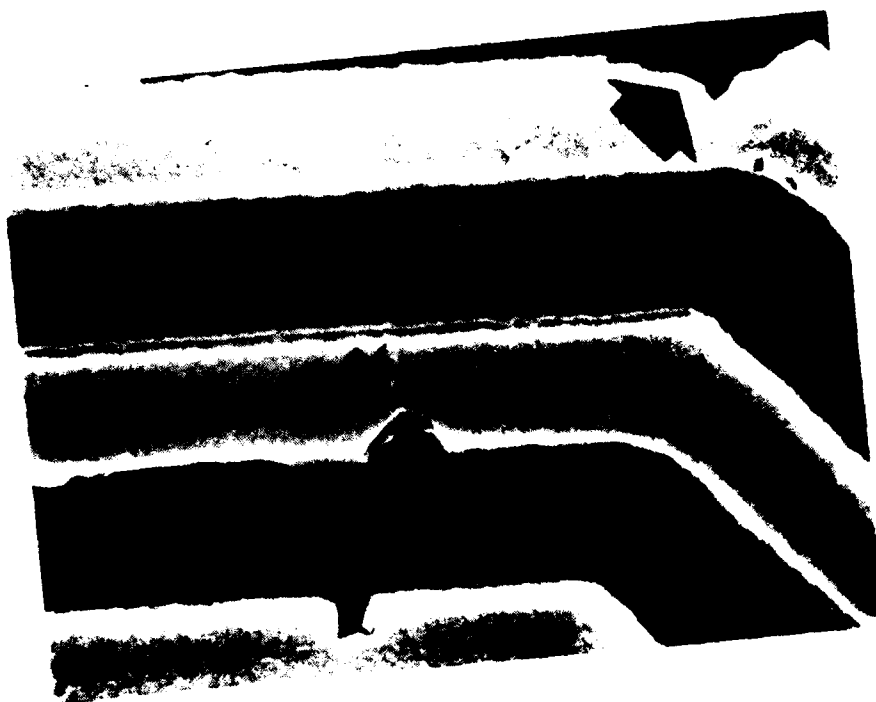


Figure 2. Half of cross sectional area restricted by metal void (SEM, after passivation removal).

3.0 THERMOMECHANICAL STRESS THEORY

The thermal coefficient of expansion mismatch between aluminum-silicon metallization, silicon nitride passivation, silicon dioxide dielectric, and silicon substrate induces a significantly large tensile stress within the metallization after a decrease in temperature (from passivation deposition to room temperature). Typical material properties used for the stress modeling are shown in Table 1. Several other properties are necessary for finite element stress modeling : Poisson's ratio, shear modulus, plastic modulus, yield strength, and creep rates. These properties are explained further in the Appendix.

TABLE 1. Typical Material Properties.

	MODULUS OF ELASTICITY (GPascals)	THERMAL COEF. OF EXPANSION (ppm/deg C)
SILICON SUBSTRATE	131.0	2.3
AL-SI METALLIZATION	70.3	23.5
SILICON NITRIDE	89.6	2.2
SILICON DIOXIDE	79.9	0.5
All material properties shown are at 25°C for simplicity purposes.		

If the tensile stress rises above the yield stress of the metallization, any additional stress will be relieved by vacancy creation and clustering (i.e., void formation). It appears that once voids and silicon nodules are formed due to thermal stress, the metallization may fail due to a creep mechanism.

Thin film Al-Si metallization yields at stresses less than 100 MPascals (depending microstructure and temperature). The von Mises failure theory can be applied to predict the yielding criterion [10] of the metal line at relatively low yield stresses. The effective von Mises stress is a scalar value based on all components of the stress tensor. It is also proportional to the square root of the distortion energy of the material in question. It can be mathematically expressed as follows:

$$\sigma_{eff} = \frac{1}{\sqrt{2}} [(\sigma_x - \sigma_y)^2 + (\sigma_y - \sigma_z)^2 + (\sigma_z - \sigma_x)^2 + 6(\tau_{xy}^2 + \tau_{yz}^2 + \tau_{zx}^2)]^{1/2} \quad (1)$$

σ = principal stresses along each coordinate axis

τ = respective shear stresses

This failure criterion determines the distortion energy available to activate the diffusion creep and indicate the degree of plastic deformation in the metallization.

In cases where formation of a vacancy at a source causes polycrystalline thin films to expand in the direction of an applied tensile stress, the energy of vacancy formation is decreased by the work done by the stress [11]. A schematic of vacancy flow within a grain experiencing tensile stress is shown in Figure 3.

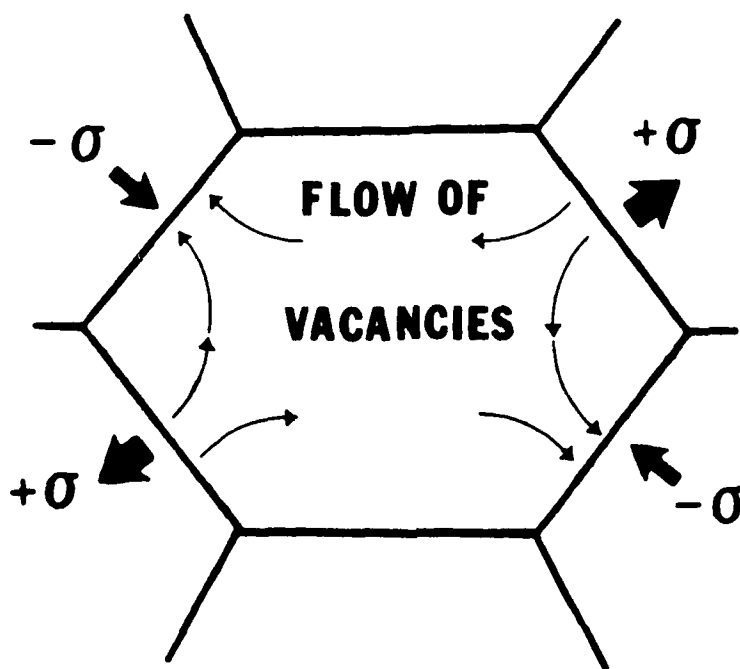


Figure 3. Schematic of vacancy flow within a grain experiencing tensile stress.

Under these conditions, vacancies flow between different sources and sinks, producing diffusional creep and subsequent voids. Using the Hall-Petch relationship, the strength of the metal line is an inverse of the grain size. If the metal line is subjected to a critical stress gradient, some net mass flow will occur in a direction to relieve the stress. Since the grain boundaries have the highest density of vacancies, migration along the grain boundaries is certainly the most rapid.

3.1 Stress and vacancy concentration

As pointed out in several Al-Si metallization studies [9], metals with a fine grain size can be deformed by the processes of vacancy (diffusion) creep. This can be by lattice diffusion of vacancies (Nabarro-Herring creep), or by grain boundary diffusion (Coble creep).

Two types of voids have been observed in the recent past [12]. One is the slit-like void which is very thin gap perpendicular to the Al-Si line edge. This type of void is the most catastrophic during failure analysis of open metallization. The other type of void is wedge-shaped which is formed along the grain boundaries at the edge of the metal lines. This void type is the result of grain boundary diffusion, whereas the slit-like void is mainly the result of lattice diffusion.

In either case a higher than normal concentration of vacancies occurs at grain boundaries transverse to a tensile stress, and a lower than normal concentration at longitudinal boundaries. This concentration gradient leads to a flow of vacancies from the transverse to the longitudinal boundaries causing an opposite of atoms that creates the tensile strain in the direction of the stress.

The gradient of vacancy concentration as a result of a tensile stress is as follows:

$$\nabla c = \frac{2 c_o(T)}{d} - \frac{\sigma b^3}{kT} \quad (2)$$

∇c = concentration gradient
 c_o = vacancy concentration (function of T)
 d = grain size
 σ = stress
 b = Burgers vector
 k = Boltzmann's constant
 T = absolute temperature

This equation yielded a Nabarro-Herring creep rate (10^{-5} sec^{-1}) with experimentally derived values [9] for low stress conditions (100 MPascals).

3.2 Stress enhanced vacancy diffusion

The diffusional creep has two major components: (1) Nabarro-Herring creep (deformation by the flow of ions through the grains) and Coble creep (deformation by ion flow in the grain boundaries). The two diffusion paths contribute in an additive sense to the strain rate as shown in the following equation:

$$\dot{\epsilon} = \frac{5 D_v}{d^2} \frac{\sigma \Omega}{kT} \left[1 + \frac{\pi \delta D_{gb}}{\delta D_v} \right] \quad (3)$$

$\dot{\epsilon}$ = diffusional creep rate
 σ = stress in metallization
 d = grain size
 δ = grain boundary width
 D_v = lattice diffusion coefficient
 D_b = boundary diffusion coefficient
 Ω = atomic volume

This equation is actually an oversimplification; it neglects the kinetics involved in detaching vacancies from grain boundary sites and reattaching them again, which may be important under certain conditions. Such behavior can become important in alloys, particularly those containing a finely dispersed second phase.

An isolated metal grain on a silicon substrate would deform to relieve thermal expansion induced stress. Since all the grains of a thin metal film are connected together, a grain boundary normal stress is generated. The grain boundary normal stress can be relieved through grain boundary migration. Metal atoms migrate from grain boundaries parallel to the stress and collect on grain boundaries normal to the stress axis. This movement relieves the stress at grain boundaries, but contributes very little to relieving the stress within individual grains.

In an unpassivated film, the edges of the line act as vacancy sinks. However, once the aluminum film is passivated with a dielectric, vacancies are trapped beneath the passivation. If these vacancies collect in one location, they will form a void. Such voids are the initial step in the formation of open metallization. Voids in a metal line locally weaken the line by developing a stress concentration around the void. At temperatures below 100 degrees C, plastic deformation is the only possible stress relief mechanism based on experimental findings. With severe stress gradients near a void, maximum deformation will be in the vicinity of the void. If the metal line is then subjected to subsequent temperature cycles below the recrystallization temperature of the metal, the metal around the void will become locally work-hardened and eventually break.

Under conditions of biaxial stress, characterizing diffusion is considerably more complex than uniaxial stress. In cases where the formation of a vacancy at a source causes polycrystalline thin films to expand in the direction of an applied tensile stress, the energy of vacancy formation is decreased by the work done by the stress; the equilibrium vacancy concentration is correspondingly increased.

In the case of hydrostatic pressure (imposed by a compressive passivation layer), a decrease in the self-diffusion rate along grain boundaries may result, but biaxial stresses in the metal film will cause intragranular vacancy diffusion to occur from boundaries in tension to boundaries in compression. All stress modeling results have indicated that there does exist a characteristic biaxial stress at the upper

corner and along the edge of the aluminum line.

Stress relaxation can take place through a number of mechanisms [13], but diffusional creep in the bulk or grain boundaries is the overriding mechanism for void formation. It follows that the stress relaxation mechanism depends strongly on the film deposition technique (grain size, texture, interfacial structure) and conditions (defects and composition).

4.0 MODELING RESULTS

Based on the thermomechanical theory and experimental observations, the numerical analysis technique of finite element analysis is used to simulate thermally-induced stresses in a localized model of passivation, metallization, oxide, and silicon layers. Appropriate boundary conditions allowed a localized analysis of the structure within 10 microns of the chip surface.

4.1 Finite element modeling fundamentals

The concept of finite element stress modeling is that a boundary-value problem can be broken down into a finite number of regions. Since the method may be applied to individual discrete elements of the continuum, each element may be given distinct physical and material properties. This approach allows one to achieve very general descriptions of the continuum.

The initial step in performing an elastic-plastic analysis is to select a yield criterion. The criterion defines how the materials respond to applied loads. The Al-Si metallization material data is assumed to obey the von Mises distortion energy theory [14].

The next step is to define a plastic-flow rule (i.e., plastic stress-strain relation). The plastic-flow rule defines how individual components of plastic strain depend on the stress components and temperature histories. In this program, the plastic strain increment is assumed to follow the Normality principle of plasticity [15].

Due to lack of supportable material data for Al-Si metallization, the validation of the foregoing assumptions applied to the metallization is unknown. However, this set of assumptions has been proved to work well for metals used in bulk form.

The final step in performing an elastic-plastic analysis is to solve a system of simultaneous nonlinear equations [16]. Since the plastic strain depends on the state of stress and the history of the thermal loading, the response calculation is effectively determined using a step by step incremental analysis. For each temperature increment, an equilibrium

condition is achieved by an iterative technique.

4.2 Application of finite element modeling

Void generation in Al-Si metallization has been observed as a result of thermomechanical stresses induced after deposition of a highly compressive passivation. In order to explain the observed experimental results, a model was developed to calculate stresses in Al-Si metallization with various widths (1-10 microns), over oxide topography, with silicon nodules, and various magnitudes of compressive passivation stresses (400-1000 MPa).

Stress induced in an Al-Si metal line is a function of (1) parameters of passivation deposition, (2) thermal coefficient of expansion of each material, (3) form factors of the multilayered structure, and (4) the intrinsic stress of each thin film structure.

The stresses in the multilayered structure are based on the following assumptions: (1) each layer adheres perfectly to adjacent layers, (2) both thermal and intrinsic stress values were essential for stress simulation, and (3) the thermal stress is calculated from a zero stress state at passivation deposition to room temperature.

An analytical approach for the calculation of the stress values during cooling after passivation deposition is not appropriate because of the material nonlinearities due to temperature-dependent plasticity and creep. The finite element method is a useful tool, especially for structures with more complicated geometry. In this stress analysis, the material model is described to be isotropic, homogeneous, and thermo-elastic-plastic in nature. All material properties are temperature-dependent; Young's modulus, E , Poisson's ratio, ν , material yield stress, σ_y , strain hardening modulus for linear strain hardening, E_T , the instantaneous coefficient of thermal expansion, α . Since the plastic stress in the metallization is a power function of the plastic strain, a rough approximation for the strain hardening modulus, E_T , was used for each temperature increment.

The essence of this material model is that constitutive law for an isotropic, thermo-elastic-plastic material will be formulated as follows:

$$\sigma = C_E (\epsilon_T - \epsilon_P - \epsilon_{th}) \quad (4)$$

- σ = stress in metallization
- C_E = component of elastic constitutive tensor defined by Young's modulus and Poisson's ratio
- ϵ_T = total strain component
- ϵ_P = plastic strain component
- ϵ_{th} = thermal strain component

Using Equation 4, the stress in the metallization can be calculated as a function of temperature, geometry, and material property variations.

In the stress model, it is assumed that the metallization possesses nonlinear material properties (plasticity, creep, etc.), and stress values are obtained using the finite element modeling program ADINA and analytical solutions under plane strain/stress conditions. The finite element mesh describing the geometry of the stress model is shown in Figure 4.

The potential for the usage of several creep laws does exist, but the current stress model does not utilize this option. In order to utilize this law, further research must be conducted for the following reasons: (1) the type of creep law which is applicable at a given temperature and stress must be determined and (2) the constants used in each appropriate creep law must be extrapolated from experimental data.

Stress modeling results show stress concentrations develop in the region of an oxide step, in the top edge of a metal line, and in the vicinity of silicon precipitates.

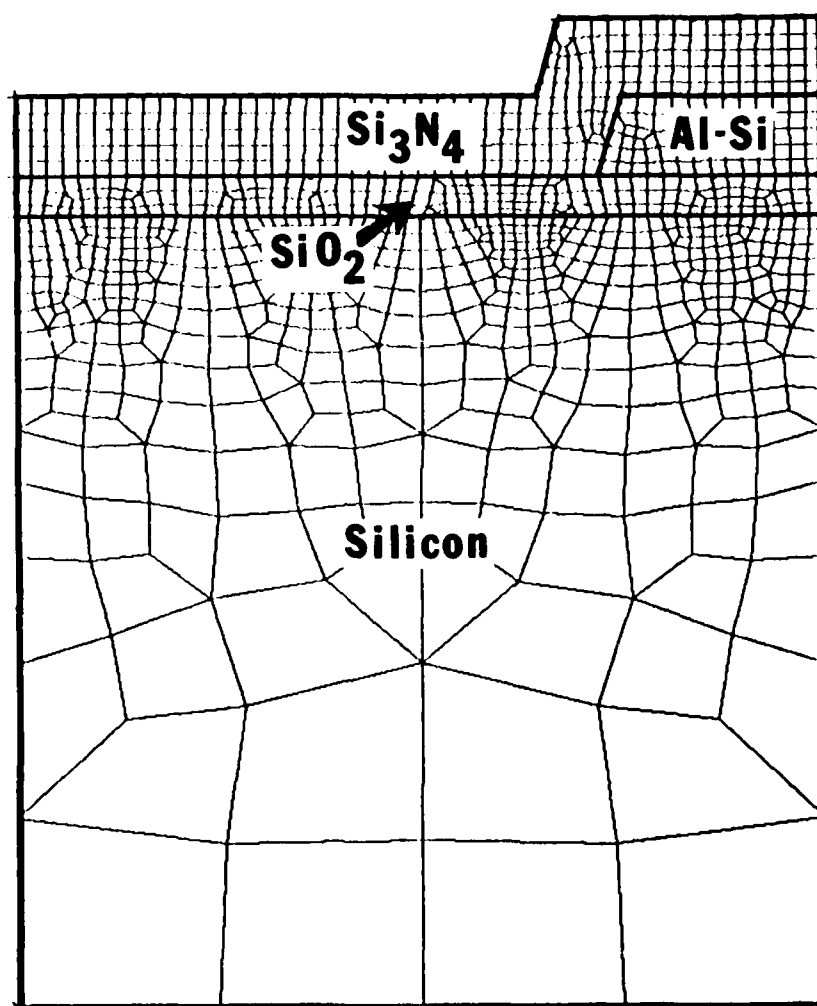


Figure 4. Finite element mesh describing stress model geometry.

4.3 Effects of underlying oxide layer

The stress models of metallization systems with varying oxide stress and thickness have been completed. Based on thermomechanical stress theory, the overall stress levels will be worse with oxide present because of the coefficient of thermal expansion mismatch.

Areas of inclusion, such as triple point of material (i.e., metal/oxide/protective overcoat), show significantly higher shear stresses than previous models with no underlying oxide. Based on thermomechanical stress theory, overall stress levels will be worse with oxide present because of the coefficient of thermal expansion mismatch (i.e., 0.5 ppm/deg C for thermal silicon oxide, 23.5 ppm/deg C for Al-Si metal, and 2.23 ppm/deg C for silicon nitride protective overcoat).

4.4 Linewidth dependence of stress

Modeling results indicate that a peak stress develops in the metal line at the 2 to 3 micron range based on variations in metal line width alone. Based on experimental findings, this is the region where grain boundaries parallel to the metal line edge decrease and bamboo structures are formed. This bamboo structure results in slit-like voids as reported by several research groups. Since this range of line widths is used quite frequently in VLSI technology, the stress in the metallization must be carefully monitored. The characteristic von Mises stress contours for a 1, 2, 3, 5, and 10 microns wide metal line are shown in Figures 5-9. The most critical stress concentration within the metallization is the shaded region in the upper edge of the metal line.

A comparison of maximum calculated stress values at site A in Figure 10 with the experimental observations of this phenomenon can be seen in Figure 11.

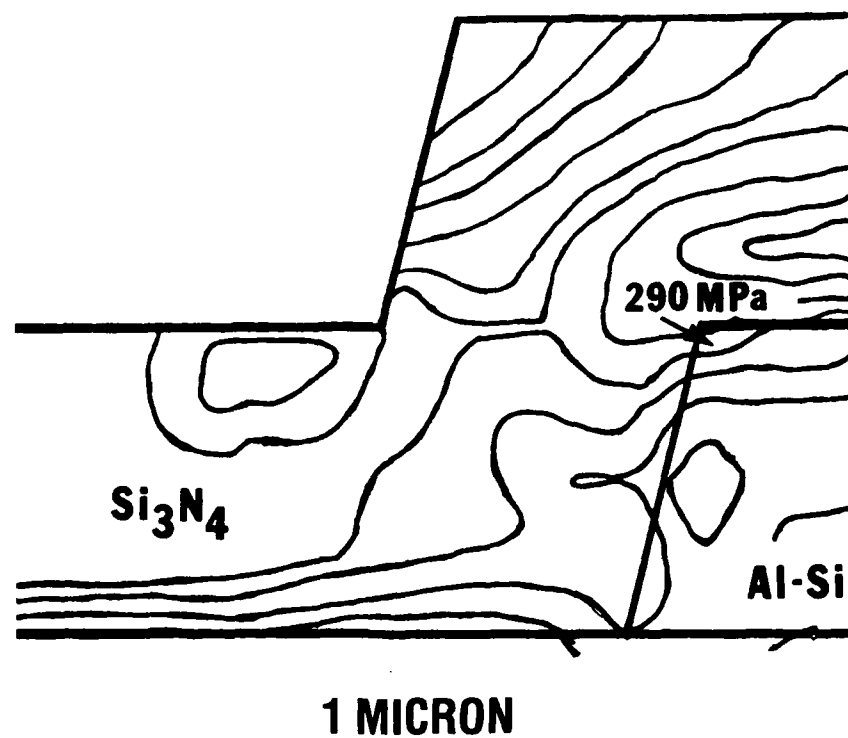


Figure 5. Von Mises stress contour plot for 1 micron wide Al-Si metal (contours at every 50 MPa).

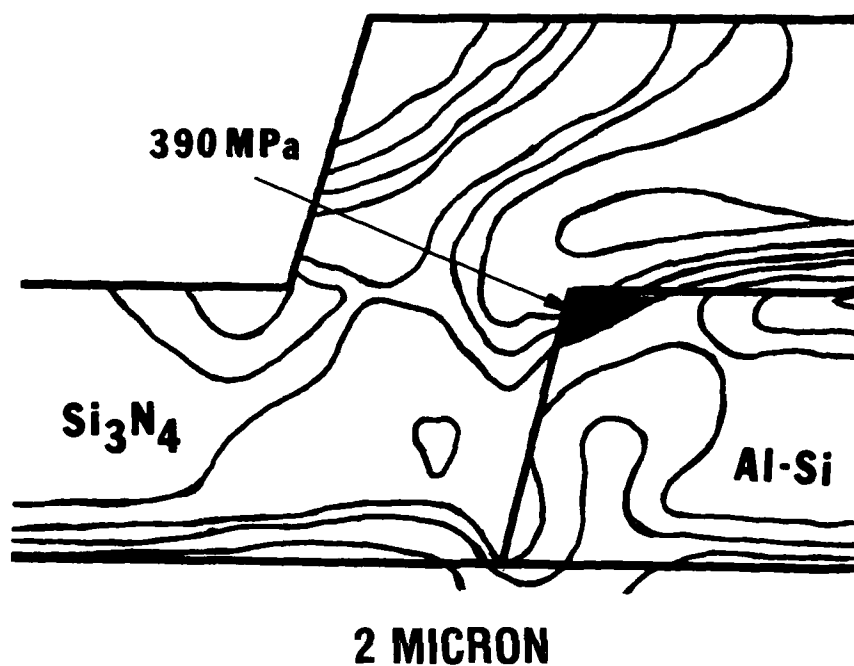


Figure 6. Von Mises stress contour plot for 2 micron wide Al-Si metal (contours at every 50 MPa).

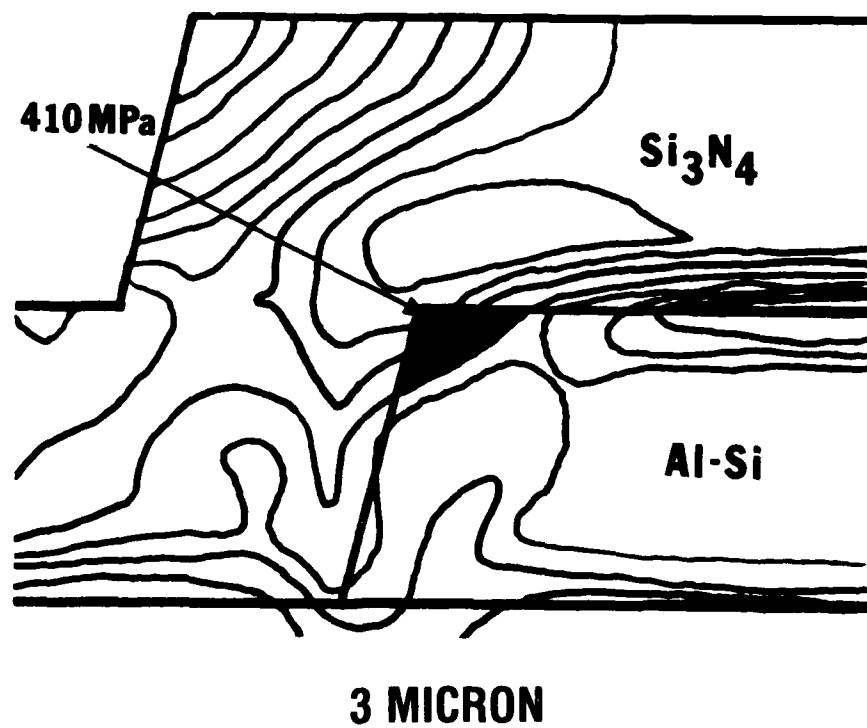


Figure 7. Von Mises stress contour plot for 3 micron wide Al-Si metal (contours at every 50 MPa).

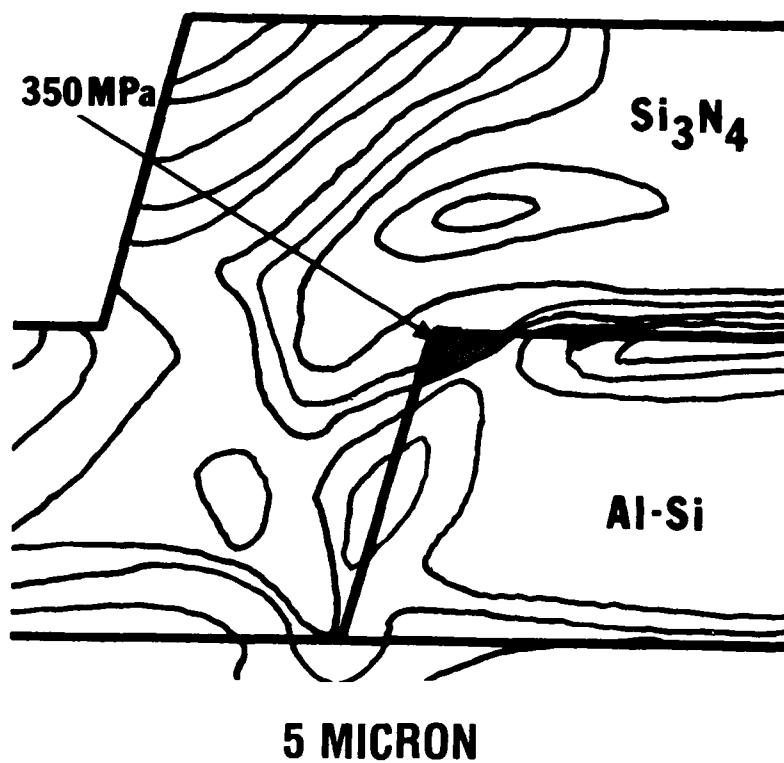


Figure 8. Von Mises stress contour plot for 5 micron wide Al-Si metal (contours at every 50 MPa).

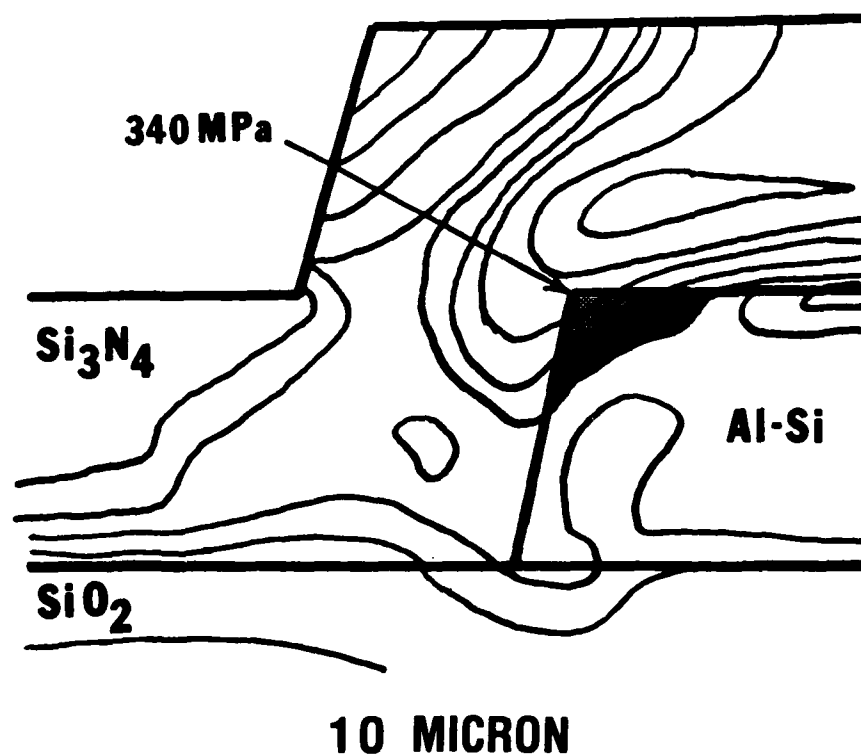


Figure 9. Von Mises stress contour plot for 10 micron wide Al-Si metal (contours at every 50 MPa).

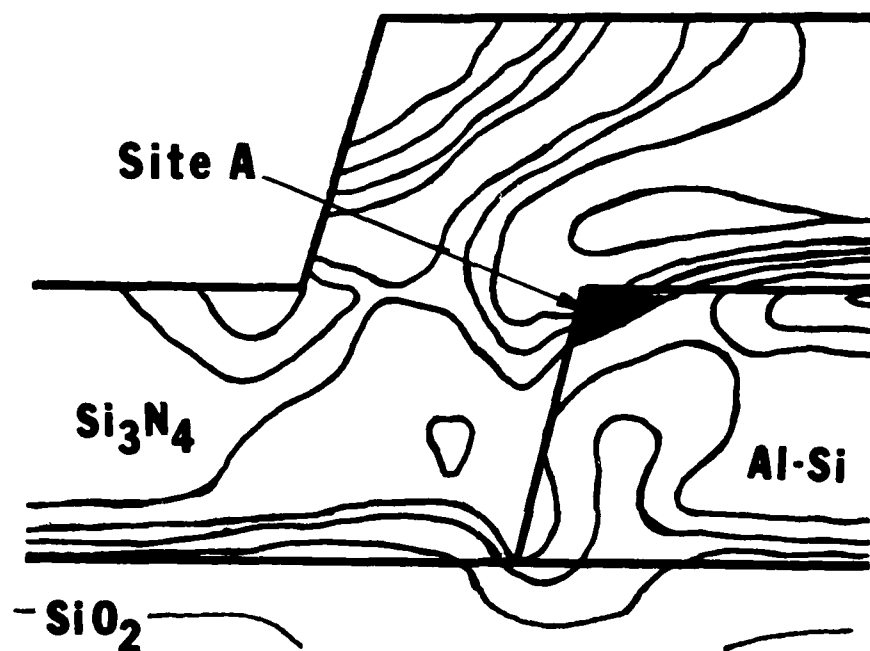


Figure 10. Typical location for maximum von Mises stress in Al-Si metallization (contours at every 50 MPa).

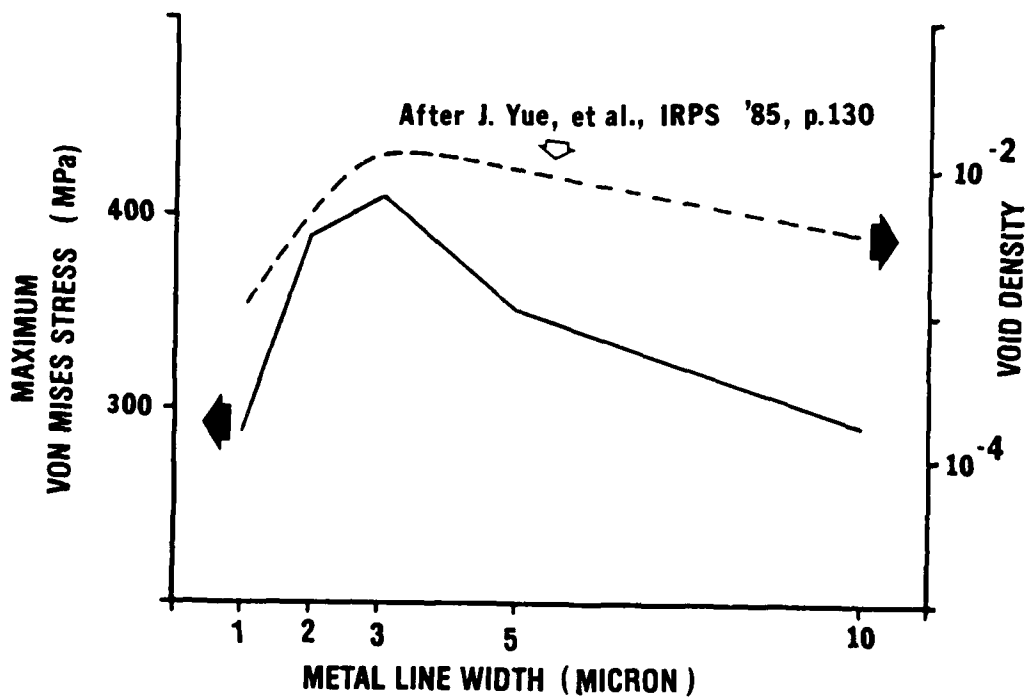


Figure 11. Comparison of theoretical stress modeling values to experimental observations².

4.5 Compressive stress passivation layer

Modeling efforts indicate that the magnitude of intrinsic stress in compressive silicon nitride passivation and its thickness is one of the most crucial factors in metal voiding/notching. Voids and notches have been observed in aluminum lines passivated with highly stressed compressive silicon nitride. The density and size of the voids are strongly dependent on the magnitude of the compressive stress in the silicon nitride passivation. The density of metal voids was found to be a power function of the tensile stress in the metallization [2]. The results suggest that a temperature-dependent transient creep is responsible for metal void formation.

There are two sources of stress in the Al-Si metallization being induced by the passivation layer. One is the stress inherent to the passivation deposition process. The magnitude of the strain in Al-Si caused by the deposition is on the order of 1 to 3 ppm, which is determined by slice curvature measurements. This value is too small to cause the voids observed in metal lines for many cases. The other source of stress is the thermal expansion mismatch between the Al-Si lines, silicon substrate, silicon dioxide layer, and passivation film. The amount of strain due to the thermal mismatch can be estimated as follows. Aluminum is essentially stress free around 400 degrees C, which is the modeled temperature of the passivation deposition process. When the metallization is cooled to room temperature, the stress formed in it is tensile. The strain induced in the metal line is calculated to be about 1% for a temperature excursion of 400 degrees C with the material properties specified in Table 1.

The characteristics of the passivation directly on top of metallization seems to be another crucial factor in minimizing metal void formation. Modeling efforts indicate that a highly compressive (greater than 400 MPa) passivation layer will induce large tensile stresses (200-500 MPa) specifically in the upper corners of the metal line. Tensile stress induced in the Al-Si metallization may also be expected to enhance grain boundary diffusivity [11].

Thicker passivation is used throughout the

semiconductor manufacturing industry to minimize damage caused by plastic packaging-related shear stress during temperature cycling. However, thicker compressive passivation produces a larger state of tensile stress in the aluminum metallization. Experimental findings [17] also indicate that the creep mechanism is thermally activated at approximately 165-180 degrees C.

4.6 Silicon nodules

Void and silicon nodule formation in Al-Si metallization are enhanced through the tensile stresses which develop in the metallization after elevated temperatures [18-21]. Silicon nodules have been found to be greater than 1 micron in size. In addition, other impurities, such as nitrogen and hydrogen, have been found in the Al-Si metallization. The failures have been either current-crowding by silicon nodules causing electromigration-like failures or increased amounts of stress in the metal lines due to the presence of silicon nodules.

The localized maximum tensile stress in a Al-Si metal line (site A in Figure 12) increases with the presence of a silicon nodule. As a result, the stress model gives physical interpretation for the initiation and growth of voids within Al-Si metallization with the presence of silicon nodules.

In many cases of open metallization, the presence of silicon nodules during metal void formation and growth has been observed. In Figure 13, typical silicon nodule growth can be observed in partially etched Al-Si. The close proximity of silicon nodules and metal voids indicates an interdependence between the two phenomenon. Stress modeling has shown that silicon precipitates cause abnormal tensile stress concentrations in the adjacent metallization. Depending on the magnitude of temperature change, the stress concentration factor can be as high as five times the average tensile stress value. Such a stress concentration can act as an initiation site for voiding and open metallization.

As the size of the silicon nodule increases (0.5 to 2.0 microns) in the metal line, the respective maximum tensile stress in the metal increases

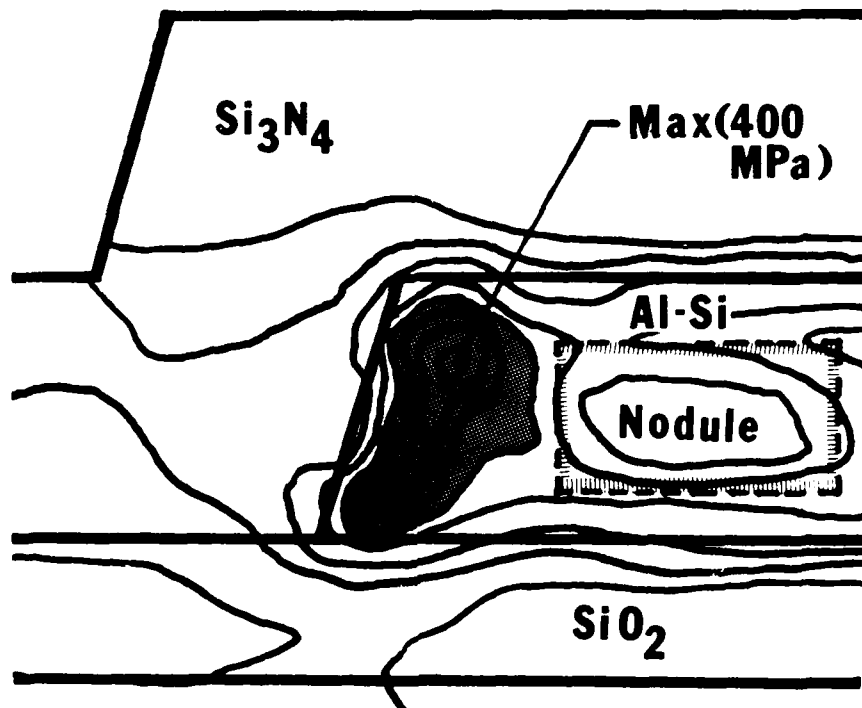


Figure 12. Maximum tensile stress contour plot for 5 micron wide Al-Si metal with presence of a silicon nodule (contours at every 50 MPa).

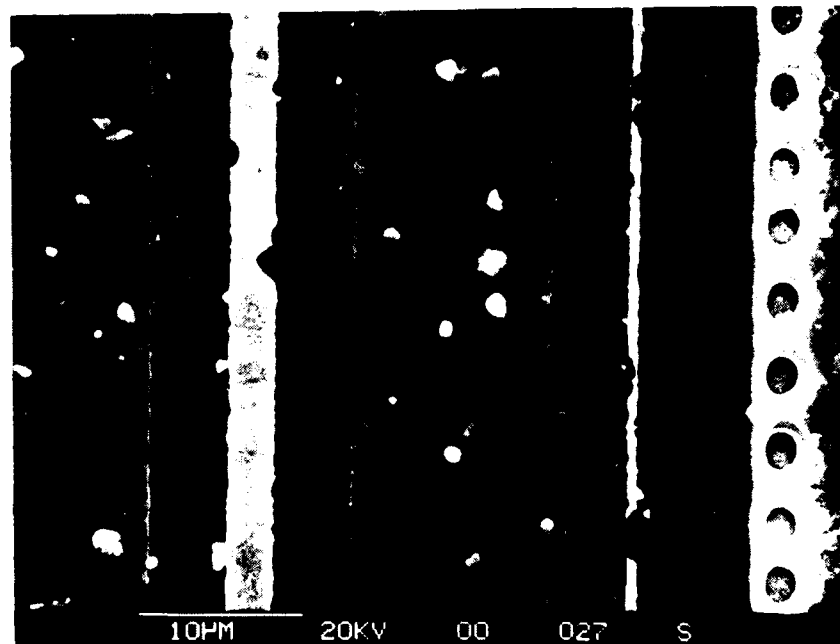


Figure 13. Proximity effect of silicon nodule and metal void formation (SEM, partially etched metallization).

significantly (10-30%) as shown in Figure 14. A graphical presentation of stress as a function of the silicon nodule size-to-linewidth ratio is depicted in Figure 15. As the cross sectional area of the silicon nodule increases, the metallization must relieve more stress per unit area. Although the von Mises stress increases at a much slower rate (5-10%), the silicon nodule can change the localized stress field dramatically during its formation. This silicon nodule formation is a dynamic process which is beyond the scope of this stress modeling program.

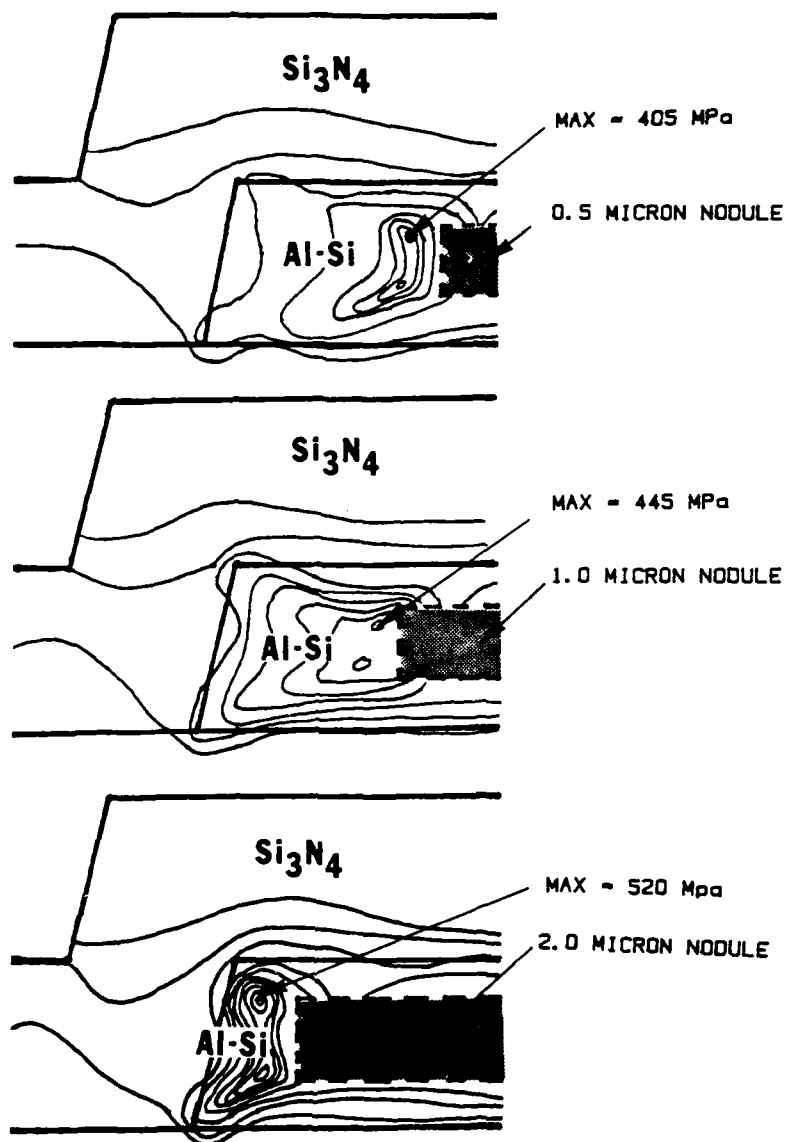


Figure 14. Induced Stress for Several Silicon Nodule Sizes (contours at every 50 MPa).

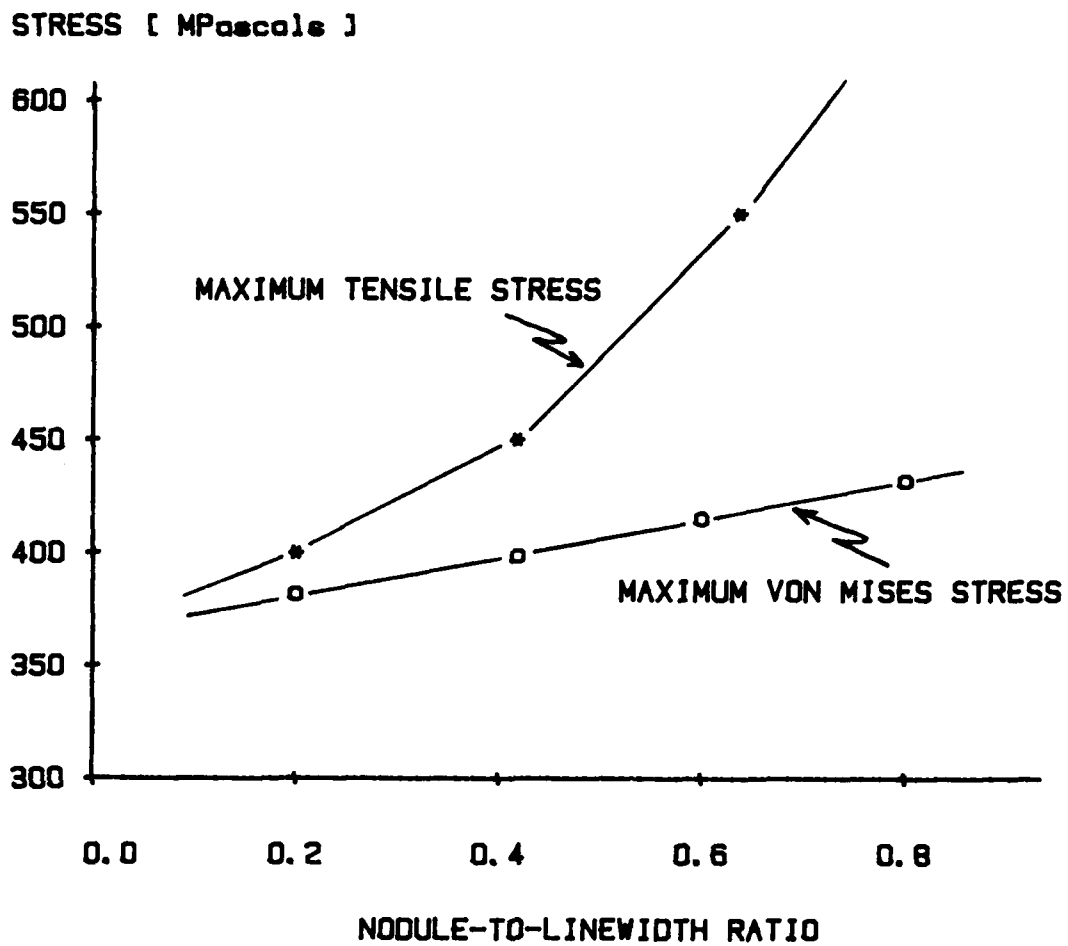


Figure 15. Maximum Tensile and Von Mises Stress as a Function of Silicon. Nodule Size-to-Line Width Ratio.

4.7 Metallization parameters

Since the mechanical and geometric properties of the metallization have a significant impact on the stress that will be induced, several parameters of the metallization are outlined below. This list of parameters is comprehensive enough to encompass key issues in open metallization failures.

4.7.1 Metal line topography

The additional stress concentration due to topography can be seen in Figure 16 (site A), as metallization traverses an oxide step. Sites of void nucleation are considered to be the combination of stress concentration areas (e.g., corners) and high levels of von Mises stress (plastic deformation failure stress). In Figures 17a and 17b, such sites are highlighted to indicate that observed voids do occur in this area more frequently. Figure 17a shows a simple two dimensional stress distribution cross section of a metal line and Figure 17b shows a cross section of a metal line over an oxide step.

Since more catastrophic open failures occur at oxide steps (Figures 18 and 19), characterizing stress as a function of the topology will aid in metal layout design. The metal void mechanism is topographically dependent: notching occurs at top surface of flat metal patterns and gross voiding, stopping at triple points in aluminum, occurs on metallization over steps. This problem is worse in ceramic packages because die attach and lid seal temperature excursions accelerate the process.

4.7.2 Variations in metal thickness

Changing the metal line thickness from 0.5 to 1.5 microns only became significant in metal linewidths less than 2 microns. Since many variations exist, only a summary of the findings are provided in this report. The calculated von Mises stress increased (10%) in a 1.5 micron thick (1 micron wide) metal line. With a 0.5 micron thick (1 micron wide) metal line, von Mises stress decreased (5%). These data points are summarized in Figure 20 which illustrates the linewidth and thickness relationship. This relationship can be seen as a form factor dependency, but must be weighted

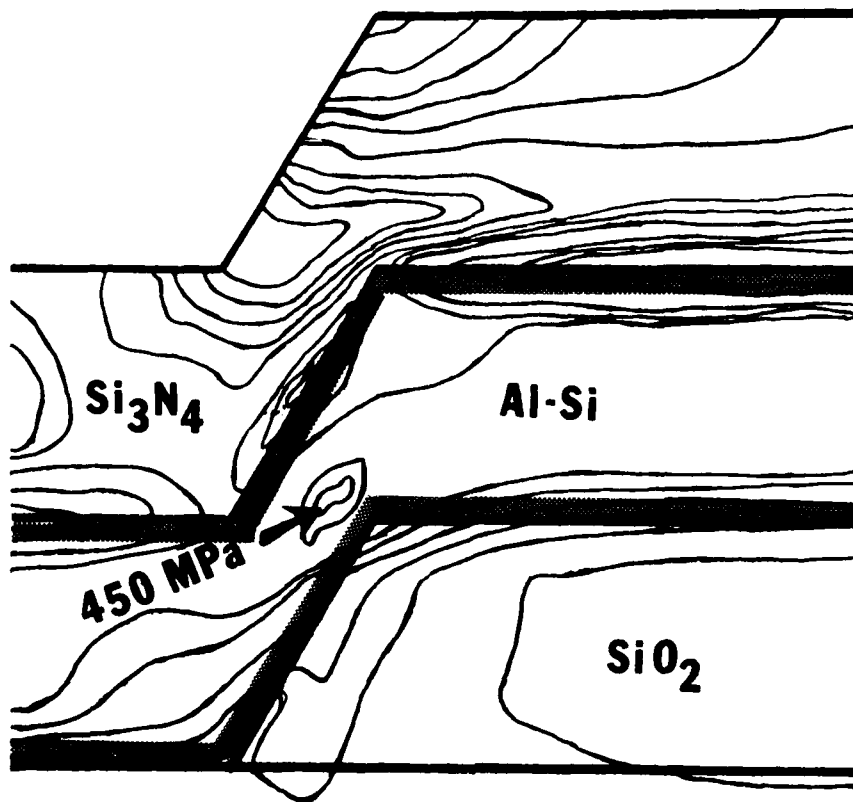


Figure 16. Maximum principal stress contour plot for Al-Si metal traversing over 1 micron oxide step (contours at every 50 MPa).

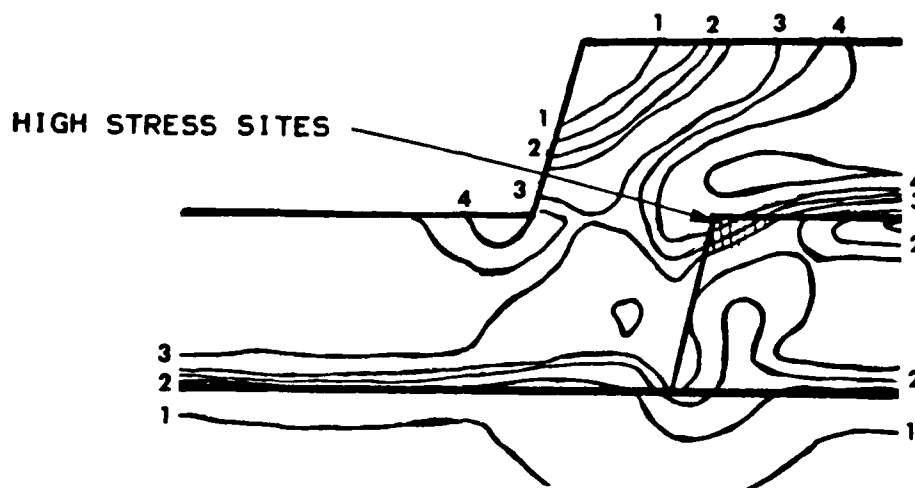


Figure 17a. Von Mises stress contour plot for 3 micron wide Al-Si metal on flat surface (contours at every 50 MPa).

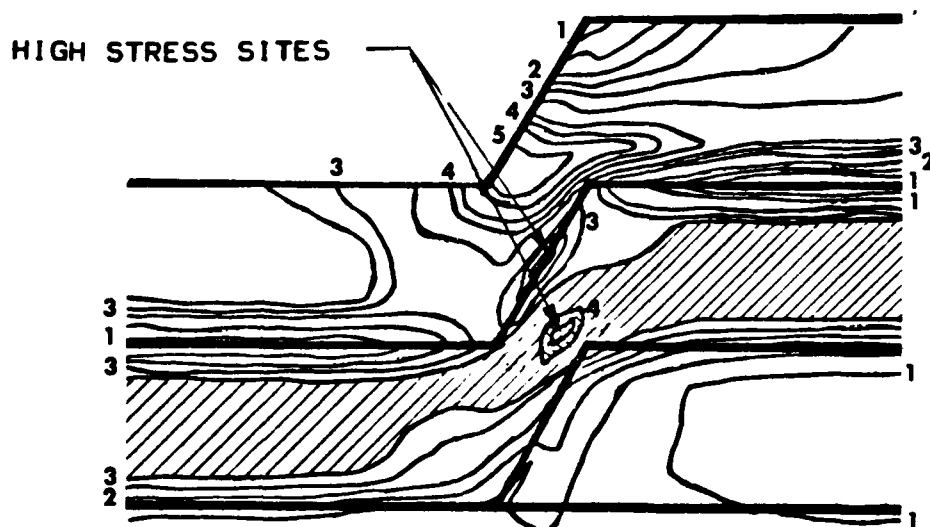


Figure 17b. Von Mises stress contour plot for Al-Si metal traversing over 1 micron oxide step (contours at every 50 MPa).



Figure 18. Metal voids observed in narrow Al-Si interconnects at oxide step (SEM, after passivation removal).

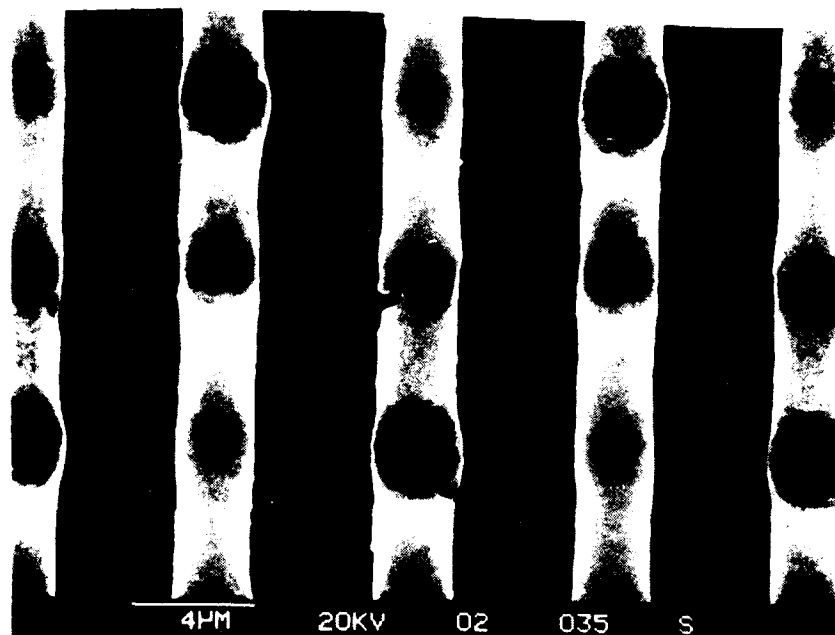


Figure 19. Metal void formation adjacent to oxide step (SEM, after passivation removal).

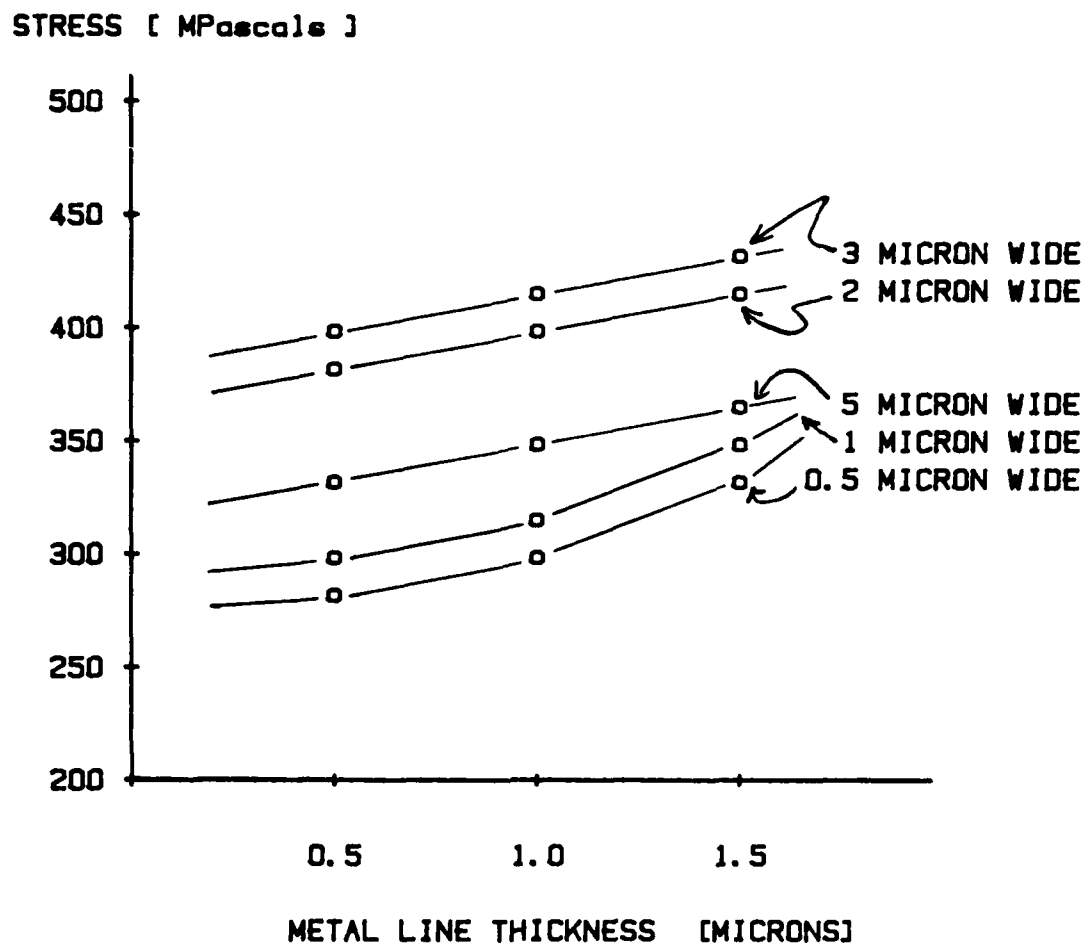


Figure 20. Maximum Von Mises Stress as a Function of Several Linewidths and Thicknesses.

with the expected grain structure and grain size expected for this linewidth in order to predict absolute void formation.

4.7.3 Metallization yield strength variations

As the yield strength of the Al-Si metallization increases (all other material properties remaining the same), the von Mises stress decreases because less plastic deformation can take place during a cooldown stage. As shown in Figure 21, a 3 micron wide metal line (yield strength at 25 degrees C = 100 MPa), the von Mises stress is approximately 410 MPa. For that same 3 micron metal line, a 50 MPa yield stress induces a 500 MPa von Mises stress and a 200 MPa yield stress induces a 350 MPa stress. A graph depicting the induced Von Mises stress in a 3 micron wide metal line as a function of metal yield strength is shown in Figure 22.

4.7.4 Metal line slant angle

Figure 23 shows variations in slant angle of metallization edge from 60 to 90 degrees. These variations cause relatively small changes in the stress produced in the metallization. The stress is simply redistributed in the metal line and shear stress in the underlying oxide changes its angle of intensity.

4.8 Aluminum-copper metal systems

Several semiconductor manufacturers have determined that with the addition of a small percentage of copper, open metallization can be minimized. Since copper rapidly precipitates out of the aluminum grain, a thin cohesive precipitate will form at the grain boundary whenever the temperature is reduced. These cohesive precipitates passivate the grain boundaries and minimize vacancy accumulation. This metal system has not been characterized well enough from a material science point-of-view to effectively model stress distributions.

4.9 Three dimensional effects

Although stress in passivation is equal in both dimensions of the metal/passivation interface plane, finite element modeling efforts indicate that the

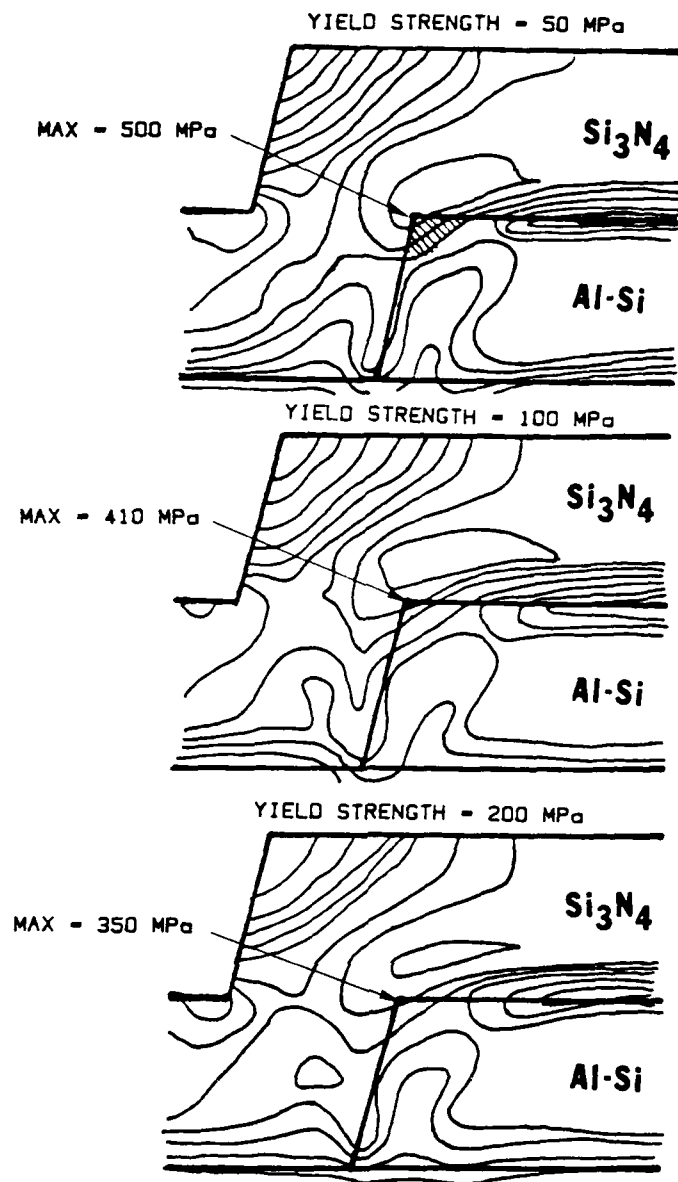


Figure 21. Induced Stress for Several Yield Strengths of Al-Si Metallization (von Mises Stress) (contours at every 50 MPa).

MAXIMUM VON MISES
STRESS
[MPASCALS]

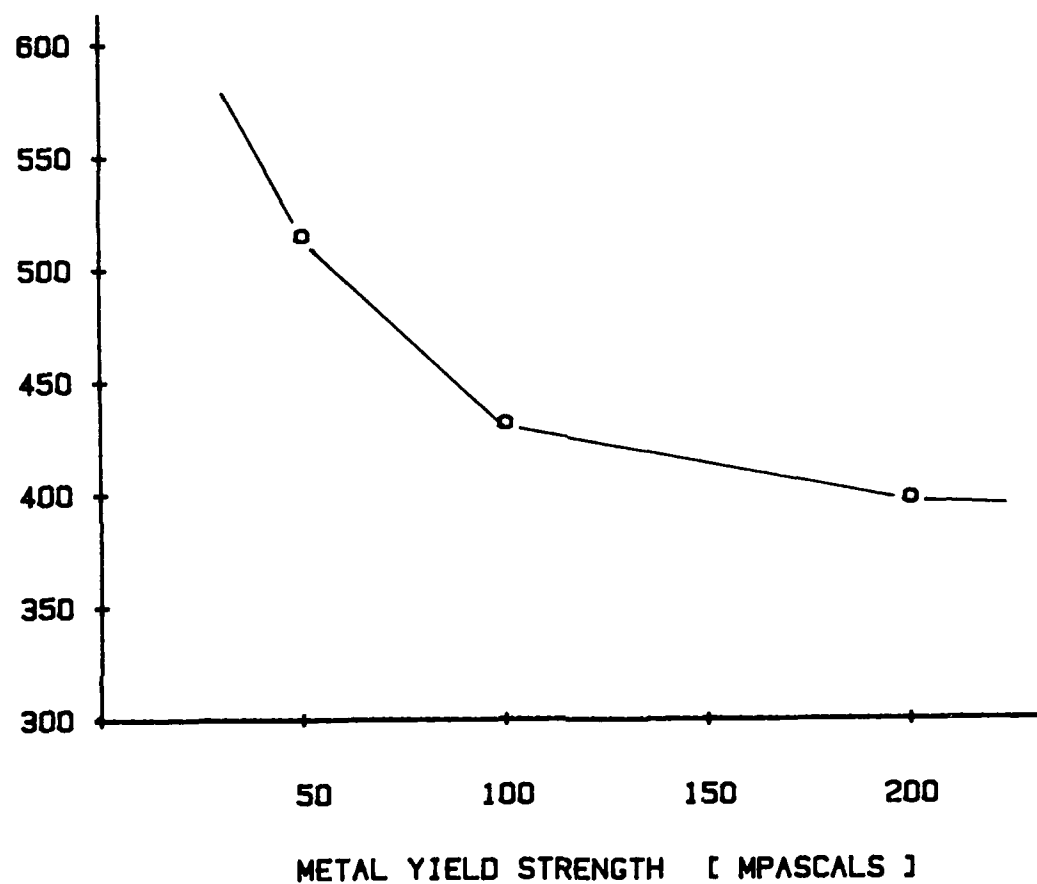


Figure 22. Maximum Von Mises Stress as a Function of Metal Yield Strength (for a 3 micron wide metal line).

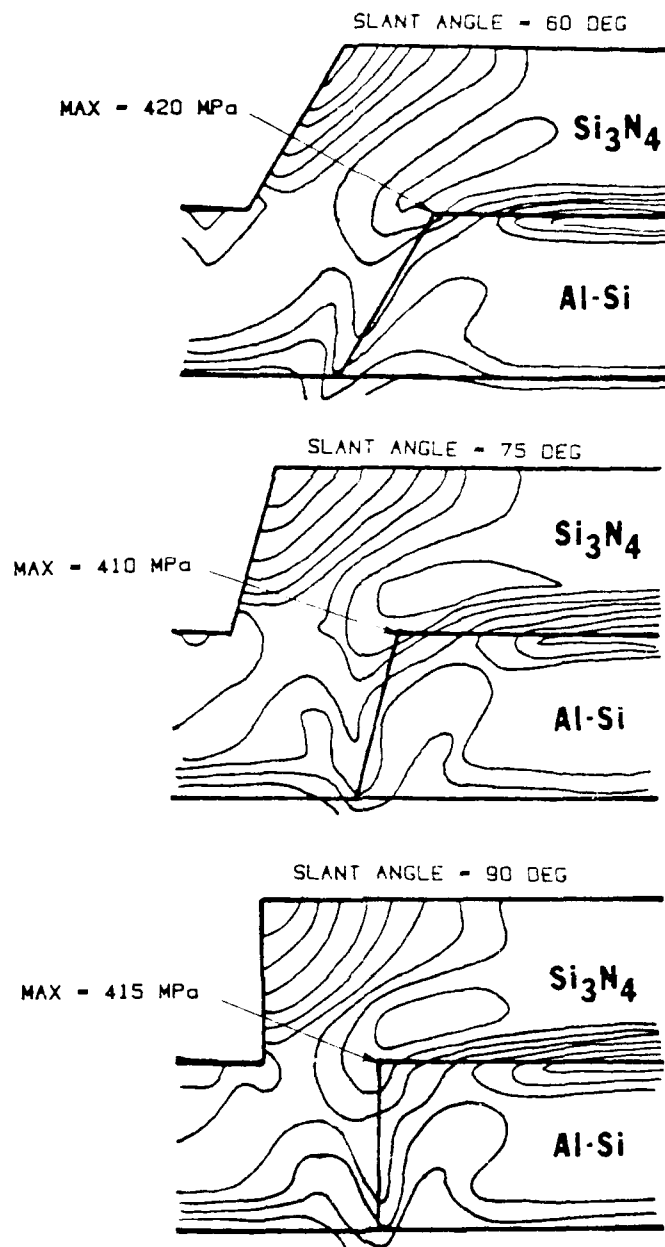


Figure 23. Induced Stress for Several Slant Angles of Al-Si Metallization Edge (contours at every 50 MPa).

stress generated by thermal expansion mismatch in the length direction can be adequately described in a two-dimensional cross-section. A view of the stress contours from a direction perpendicular to the surface are depicted in Figures 24 and 25. The strength of the metal

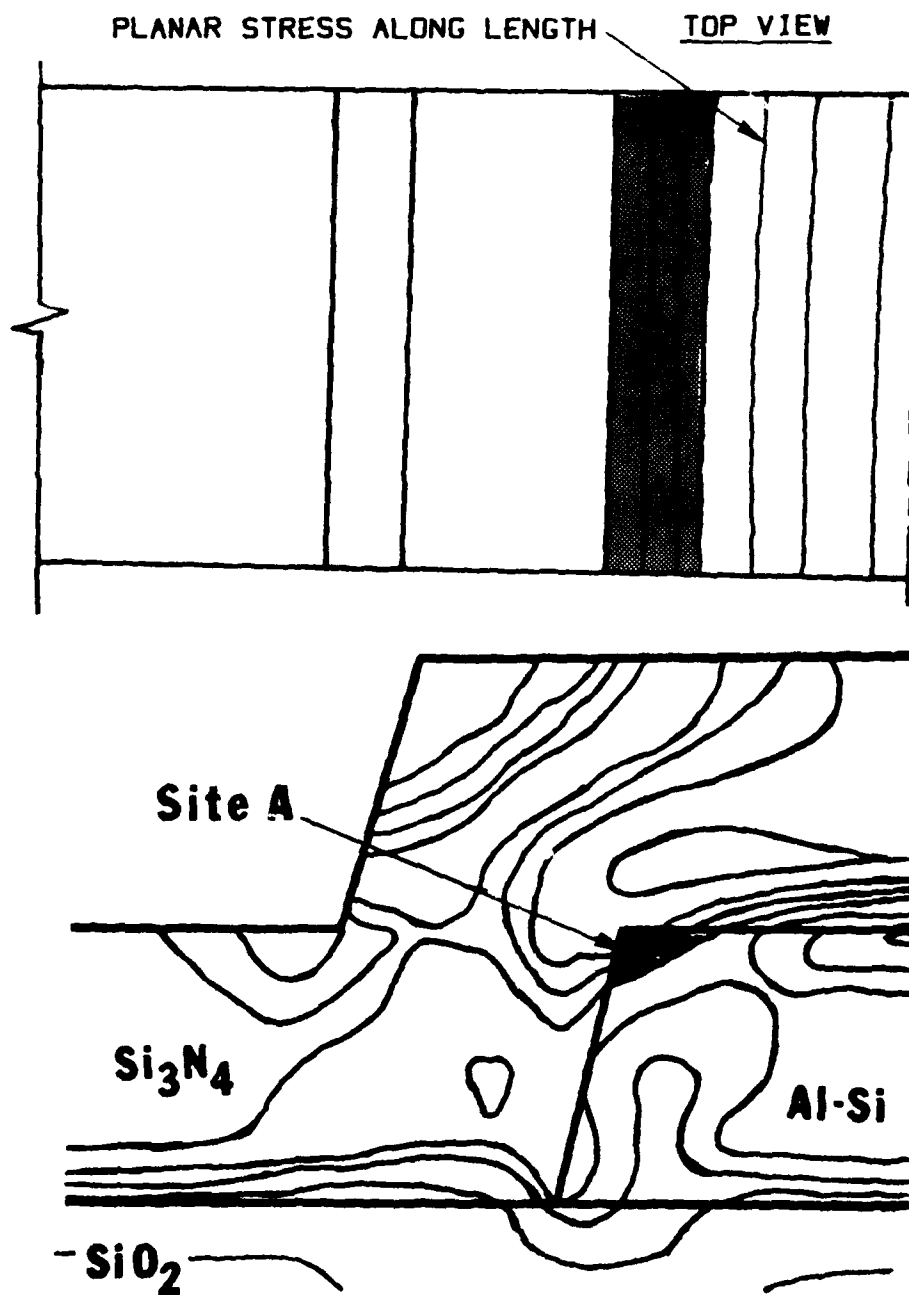


Figure 24. Three Dimensional View of Metallization Stress.

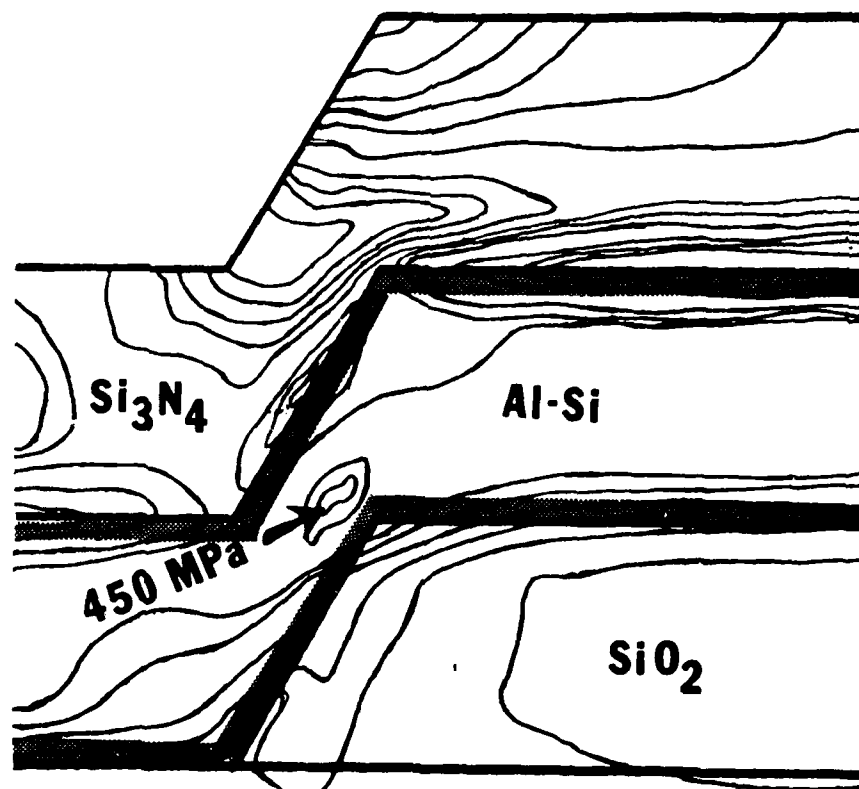
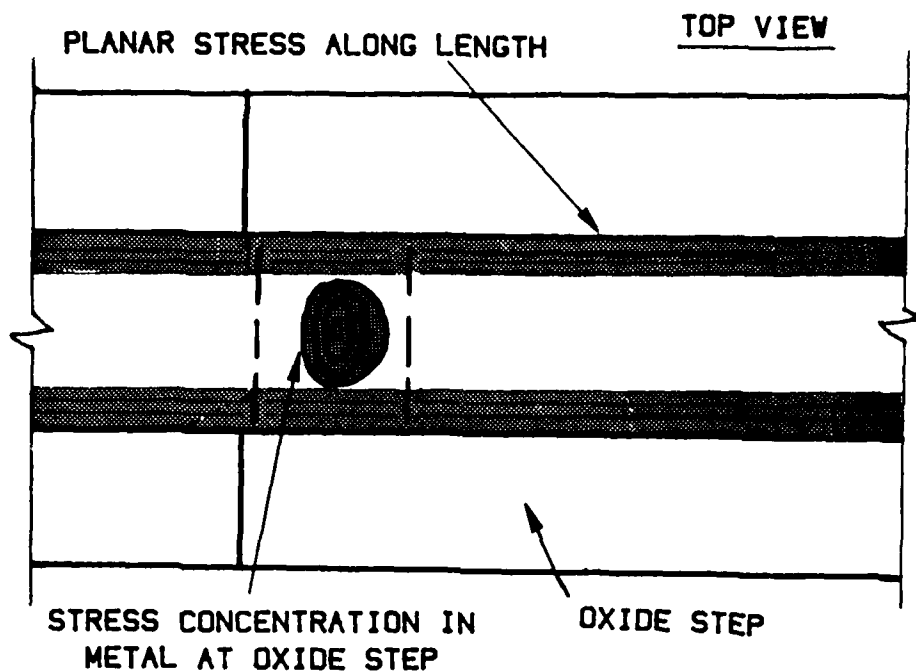


Figure 25. Three Dimensional View of Metallization Stress - Over an Oxide Step.

line is proportional to the width of the line (i.e., grain size). If the metal line is subjected to a critical stress field, some net mass flow will occur in a direction to relieve the stress. Since the grain boundaries have the highest density of vacancies, migration along the grain boundaries is certainly the most rapid.

5.0 SUMMARY AND CONCLUSIONS

To assure designed-in reliability standards, it has become necessary to semi-quantitatively determine the effects of several integrated circuit fabrication parameters on metallization stress : the metal form factors, the magnitude of allowable compressive stress in passivation layers, and the presence of silicon nodules.

The objective of the Stress Related Failures Causing Open Metallization contract was to clarify the stresses in microelectronic chips which can result in open metal failures. Based on the results of the effort, the following conclusions can be reached:

1. PHYSICAL INTERPRETATION - Through the use of numerical analysis techniques, excellent correlation with experimental observations can be achieved. As a result, the present stress model gives an adequate physical interpretation for the initiation and growth of voids within Al-Si metallization.

2. VOID INITIATION - In the presence of vacancy concentration gradients, stress fields will lead to the initial flow of vacancies from the transverse to the longitudinal boundaries. This flow will in turn, cause an opposite flow of metal atoms that creates the tensile strain in the direction of the stress. It has been shown in previous studies [22] that the preferred location for void nucleation is at the edges of the metal line. VOID GROWTH - These vacancies will cluster to form microscopic voids given sufficient time at low temperature.

3. VOID LOCATION - It has been observed throughout the semiconductor industry that voids have a preference to accumulate at the upper edge of the metal line. The stress modeling results indicate that this region has the highest stress gradients and magnitudes than any other location.

4. LINEWIDTH DEPENDENCE - Observations of peak void density in Al-Si linewidths of 2 to 3 microns have correlated well with the peak calculated thermomechanical stress in this range. There exists a form factor relationship in the stress levels of thin film Al-Si metallization. The most sensitive parameter

in this relationship is the linewidth. The second and third most sensitive parameters are the thickness and length, respectively. As seen in Figure 11, experimental data is typical of the stress values calculated by FEM. The only variable in this particular analysis was form factor related (i.e., metallization line width). A similar characteristic curve of electromigration data depicting the same type of line width dependence of electromigration lifetimes has been observed [23].

5. PASSIVATION STRESS - Experimental results have shown the effects of highly stressed silicon nitride passivation on Al-Si voiding during bake testing (greater than 100 degrees C). Observations have indicated that as the passivation stress increased from 500 MPascals to 1000 MPascals, the percentage of the void size to linewidth increased from 15% to 45% [17]. The calculated stress values in the metallization also showed a linear relationship with the stress in the passivation.

6. SILICON NODULES - The presence of silicon nodules in Al-Si metallization act as stress concentration sites and provide a supplemental tensile strain for void formation. In some cases, experimental observations reveal silicon nodules in the vicinity of large voids. The stress modeling data indicates that silicon nodules induce relatively large tensile strains in the metallization. An increase in the size of the silicon nodule also translates into larger tensile stress, and therefore a larger probability of catastrophic void formation (open metallization). Metal voids, appearing after metal and passivation deposition (through stress relaxation and creep), serve as stress concentrations. The tensile stress concentration in the vicinity causes metal voids to grow further in subsequent thermal packaging and assembly operations.

7. MATERIAL CHARACTERIZATION - This program encountered several problems with material property data of thin film materials. However, the elasticity and plasticity of the Al-Si metallization gave sufficient information regarding the relative magnitude of stress. The micromechanics and creep rate of Al-Si metallization are key parameters which remain to be

characterized well enough to be useful in the stress modeling software. This characterization must be completed before any significant stress data can be formulated.

Upon presentation of this work to the technical community, several semiconductor manufacturers have implemented finite element stress modeling to theoretically analyze stress distribution in metallization. This dissemination of techniques will eventually results in better reliability of semiconductor products.

6.0 RECOMMENDATIONS

The results of the finite element stress modeling performed during this contract were the starting point for additional metallization studies. In order to minimize the probability of void formation in Al-Si metallization, a coupling of the micromechanics of Al-Si metallization, experimental observations and stress modeling must be achieved.

This project took a "first look" at the stress distribution in thin film metallization as induced by thermal excursions. Such parameters as, thermal history of the metallization, addition of copper to the Al-Si metallization, multilevel metallization, and layered metallization (Ti/W/Al-Si) need further investigation which is beyond the scope of this project. However, this work advanced the physical interpretation of void formation in Al-Si metallization based on several boundary conditions.

Control of the metallization microstructure, silicon nodules growth, and passivation deposition processes should allow production of interconnects with improved reliability. The delicate balance in microstructure is really an issue of fabrication techniques, metal systems, electromigration requirements, and deposition parameters. The silicon nodule control is driven by the silicon content in the metallization and is defined by several fabrication techniques. A minimization of nodules will increase the mechanical integrity of the metallization significantly. The magnitude of compressive stress in the passivation layer is basically a function of the deposition parameters: the Si/N ratio, hydrogen bonding, the density and the related microstructure of the film. Minimization of the compressive stress level in the passivation in order to decrease the induced tensile strain in the metallization must be weighted against the pinhole integrity of the passivation. Both experimental and modeling results indicate that compressive stress levels in the passivation must be less than 1000 MPascals, in order to avoid open metallization failures.

REFERENCES

- [1] T. Turner and K. Wendel, "The Influence of Stress on Aluminum Conductor Life," IEEE Proc. 23rd Annual Proc. Rel. Phys., pp. 142-147, 1985.
- [2] J.T. Yue, et al., "Stress Induced Voids in Aluminum Interconnects During IC Processing," IEEE Proc. 23rd Annual Proc. Rel. Phys., pp. 126-137, 1985.
- [3] M.R. Lin and J.T. Yue, "Impact of Ceramic Packaging Anneal on the Reliability of Al Interconnects," IEEE Proc. 24th Annual Proc. Rel. Phys., pp. 164-171, 1986.
- [4] N. Owada, et al., "Stress Induced Slit-Like Void Formation in a Fine-Pattern Al-Si Interconnect During Aging Test Proceedings," IEEE VLSI Multi-Level Interconnect Conference, pp. 173-179, 1985.
- [5] K. Hinode, et al., "Stress-induced Grain Boundary Fractures in Al-Si Interconnects," J. Vac. Sci. Technol. B 5 (2), pp. 518-522, 1987.
- [6] H. Koyama, et al., "Suppression of Stress Induced Aluminum Void Formation," IEEE 24th Annual Proc. Rel. Phys., pp. 24-29, 1985.
- [7] J. Klema, et al., "Reliability Implications of Nitrogen Contamination During Deposition of Sputtered Aluminum/Silicon Metal Films," IEEE 22nd Annual Proc. Rel. Phys., pp. 1-5, 1984.
- [8] H. Hieber, "Thermomechanical Relaxation of Thin-Film Metallizations," Material Research Society Symposium Proceedings, 40, pp. 191-202, 1985.
- [9] H. Hieber and T. Simon, "Thermo-mechanical Cycling Behavior of Al Thin-Film Metallization," IEEE Proc. 24th Annual Proc. Rel. Phys., pp. 253-259, 1986.
- [10] R.E. Jones, Jr., "Line Width Dependence of Stresses in Aluminum Interconnect," IEEE Proc. 25th Annual Proc. Rel. Phys., pp. 9-14, 1987.

- [11] R.W. Balluffi and J.M. Blakely, "Special Aspects of Diffusion in Thin Films," Thin Solid Films, 25, pp. 363-392, 1975.
- [12] S. Mayumi, et al., "The Effect of Cu Addition to Al-Si Interconnects on Stress Induced Open-Circuit Failures," IEEE Proc. 25th Annual Proc. Rel. Phys., pp. 15-21, 1987.
- [13] M. Hershkovitz, et al., "Stress Relaxation in Thin Aluminum Films," Thin Solid Films, 130, pp. 87-93, 1985.
- [14] T. Z. Blazynski, "Applied Elasto-Plasticity of Solids," London, Macmillan, 1983.
- [15] W. Prager, "Introduction to Mechanics of Continua," Boston, Ginn, 1961.
- [16] J.T. Oden, "Finite Elements of Nonlinear Continua," New York, McGraw-Hill, 1973.
- [17] C.F. Dunn and J.W. McPherson, Private communication.
- [18] S.J. O'Donnell, et al., "Silicon Inclusions in Aluminum Interconnects," IEEE 22nd Annual Proc. Rel. Phys., pp. 9-16, 1984.
- [19] T. Tatsuzawa, et al., "Si Nodule Formation in Al-Si Metallization," IEEE 23rd Annual Proc. Rel. Phys., pp. 138-141, 1985.
- [20] J. Curry, et al., "New Failure Mechanisms in Sputtered Aluminum-Silicon Films," IEEE 22nd Annual Proc. Rel. Phys., pp. 6-8, 1984.
- [21] S.B. Herschbein, et al., "Effects of Silicon Inclusions on the Reliability of Sputtered Aluminum-Silicon Metallization," IEEE 22nd Annual Proc. Rel. Phys., pp. 134-137, 1984.
- [22] R.W. Pasco, et al., "The Effects of Hydrogen Ambients on Electromigration Kinetics in Al-2%Cu Thin Film Conductors," Solid-State Electronics, pp. 1053-1063, 1983.

- [23] S. Vaidya, et al., "Electromigration Resistance of Fine-Line for VLSI Applications," IEEE 18th Annual Proc. Rel. Phys., pp. 165-170, 1980.

1.4 Stress model scaling

Extensive computation time would be necessary if the model included the entire die and the thin film structures. The thickness of the silicon substrate was significantly reduced while maintaining the same stiffness. Therefore, the model was scaled down to include only thin film structures and a small portion of the silicon substrate.

The finite element mesh (Figure 4, main text) was generated with careful consideration of the transition from macroscopic to microscopic features by (1) including boundary conditions which maintained the same stiffness of the entire chip, (2) maintain an aspect ratio of 3 to 1 for all elements in the model, and (3) requiring material interfaces to be continuous. Based on these assumptions, the stress model used throughout the project was considered to be appropriate for this stress simulation.

The symmetry of the model permitted the use of only one-half of the multilayered structure during model creation and analysis phases which significantly decreased the computational time.

2.0 MODELING RESULTS

Due to the computational nature of finite element analysis and the vast amount of output for single simulations, the stress contour diagrams have been included in the text of this report. It is quite clear in reviewing the stress contour plots that the stresses in the metallization are relatively high at the upper edge of the metal line.

The thermally-induced stresses are extremely complex tensor quantities which are difficult to represent in a standard plot. Since plastic deformation occurs past the elastic limit (von Mises failure theory), the most useful plot would be that of von Mises stress. This is an energy-related stress and has been determined for all variables in this contract. With a constrained metallization, this plastic flow only results in small strain deformations which allow stress relaxation. The calculated stresses are tensile, as expected by simple thermomechanical stress theory.

END

DATED

FILM

8-88

Dtic